Harziphilone and Fleephilone, Two New HIV REV/RRE Binding Inhibitors Produced by *Trichoderma harzianum*

JINGFANG QIAN-CUTRONE*, STELLA HUANG, LI-PING CHANG, DOLORES M. PIRNIK, STEVEN E. KLOHR, RICHARD A. DALTERIO, ROBERT HUGILL, SUSAN LOWE, MASUD ALAM and KATHLEEN F. KADOW

Bristol-Myers Squibb Pharmaceutical Research Institute, 5 Research Parkway, Wallingford, Connecticut 06492, U.S.A.

(Received for publication July 15, 1996)

During the screening of the natural products for their ability to inhibit the binding of REV (regulation of virion expression) protein to [^{33}P] labeled RRE (REV responsive element) RNA, two novel fungal metabolites, harziphilone and fleephilone, were isolated from the butanol-methanol (1 : 1) extract of the fermentation broth of *Trichoderma harzianum* by bioassay guided fractionation. The structures of these two new compounds were established by spectroscopic methods. Harziphilone and fleephilone showed inhibitory activity against the binding of REV-protein to RRE RNA with IC_{50} values of 2.0 μM and 7.6 μM, respectively. However both compounds did not protect CEM-SS cells from acute HIV infection at concentration levels up to 200 μg/ml using an XTT dye reduction assay. In addition, harziphilone demonstrated cytotoxicity at 38 μM against the murine tumor cell line M-109.

Replication of human immunodeficiency virus (HIV) is dependent upon many specific interactions between viral RNAs and proteins of viral and cellular origin. REV (regulation of virion expression) is an HIV protein that regulates the transport of viral RNA to the cytoplasm, thus, it is essential for HIV productive infection. The interaction of the basic domain of REV with the REV-responsive element (RRE), a stem loop RNA structure in the envelope region, is required for REV function[1~3]. Inhibitors of this interaction could be of use as anti-viral agents. Therefore we developed a high-throughput screen to identify inhibitors of the formation of this REV/RRE complex. Activity of the REV active compounds against HIV was studied with a cell protection, XTT dye reduction, assay.

During the screening of natural products for their ability to inhibit the binding of REV protein to RRE RNA, the butanol extract of *T. harzianum* WC47695 was found to be active. When subjected to bioassay-guided fractionation, two novel active fungal metabolites, designated as harziphilone (**1**) and fleephilone (**2**), were isolated (Fig. 1). This report describes the fermentative production, isolation, structure elucidation and biological activities of these two compounds.

Materials and Methods

Taxonomy

The fungal strain WC 47695, was isolated from sandy soil with plant debris collected in Fort Lauderdale, Florida. This culture produces colonies on Potato Dextrose agar and Malt Extract agar, which are fast spreading with aerial hyphae appearing within 48 hours of incubation at 28°C. Conidial areas appear after 3 days as dull green floccose growth with a colorless reverse. Hyphae are branched, smooth-walled and hyaline. Conidiophores are ramified with side branches appearing long and slender without sterile hyphal elongations. Phialides are regularly spaced, not crowded, appearing in groups of 4~5 and also singly on smaller branches. They are flask-shaped measuring an average of 5.5 × 3.4 μm. Phialospores are produced singly, accumulating at the tip of the phialide forming a rounded conidial head. They are globose to subglobose, smooth-walled

Fig. 1. Structures of harziphilone (**1**) and fleephilone (**2**).

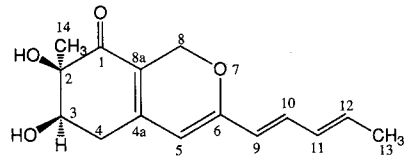

Harziphilone (1)

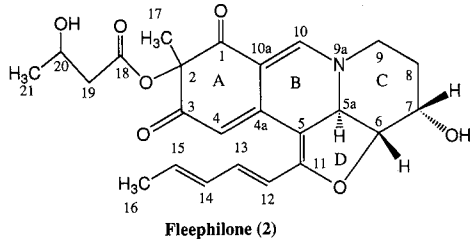

Fleephilone (2)

and measure an average of 2.3 μm in diameter. They are pale green when viewed singly but appear much darker in mass[4,5]. Based on the arrangement of conidiophores and phialides and in the size of its phialospores, this culture is classified as *Trichoderma harzianum*.

Fermentation

T. harzianum was grown on a PDA slant for 7 days at 28°C, and 6 ml of 20% (w/v) glycerol was added and used to prepare a spore suspension, which was divided into aliquots, frozen in a dry ice-acetone bath, and stored at −80°C. From the frozen stock, 0.1 ml was used to inoculate a PDA stant which was incubated at 28°C for 7 days, before being transferred into 100 ml of fresh medium in a 500 ml flask, using a sterile swab. The medium contained the following per liter of distilled water: glycerol, 30 g; glucose, 20 g; polypeptone, 5 g; yeast extract, 3 g; NaCl, 3 g; $CaCO_3$, 5 g. The culture was grown for 3 days at 26°C at 250 rpm on a gyrotary shaker and 4 ml was used to inoculate 100 ml of the same medium, which was also used as the production medium. The culture was incubated for 6 days at 26°C at 250 rpm and samples taken at intervals for determination of inhibitory activity in the REV/RRE binding assay.

Extraction and Isolation

The fermentation broth (10 liters) was divided into filtrate and mycelia by filtration. The filtrate was stirred vigorously with 1-butanol (3 liters) and MeOH (3 liters) for 1 hour. The 1-butanol/MeOH extract was evaporated *in vacuo* to dryness. The residue (2.1 g) was dissolved in 90% aq. MeOH (222 ml) and then partitioned with hexane (3 × 222 ml). The aq MeOH layer was diluted with 86 ml of water to a 65% MeOH solution and partitioned against pre-equilibrated chloroform (3 × 200 ml). The $CHCl_3$ layers were pooled and evaporated to give a crude solid (912 mg). The solid was loaded to the top of a silica gel column, eluted subsequently with hexane : EtOAc (1 : 4), EtOAc and EtOAc : MeOH (9 : 1) to yield two active subfractions A (230 mg) and B (112 mg). From subfraction A, **1** (20 mg) was isolated by column chromatography on Sephadex LH-20 (MeOH) and purified by a MCI-gel CHP20P column, eluted with MeOH. The same process of subfraction B yielded **2** (11 mg).

Instrumental Analyses

The UV spectrum was taken on a Shimadzu UV2100 spectrophotometer; the IR spectrum was recorded on a Perkin Elmer FT-IR 1800 spectrometer; Electrospay mass spectra (MS) were taken on a Finnigan TSQ7000 triple quadruple mass spectrometer, the high resolution FAB-MS analysis was performed with a Kratos MS50 mass spectrometer, and all ^1H ^{13}C NMR spectra including COSY, HETCOR, COLOC and HMBC were taken on a Bruker AM-500 spectrometer (^1H, 500 MHz; ^{13}C, 125 MHz).

REV/RRE Binding Assay

REV protein was expressed in *E. coli* and prepared essentially as described previously[6]. The HIV-1 RRE region was cloned between the T7 and T3 promoters in the Blue script KS+ plasmid (Stratagene). *In vitro* transcribed, [^{33}P] radiolabeled RRE RNA was incubated with potential inhibitors and REV protein. Unless an inhibitor is present, RRE RNA forms a complex with REV protein that is then bound to nitrocellulose filters and is quantitated by liquid scintillation counting as described previously[7~9]. This assay was automated and adapted for high-throughput screening of synthetic compounds and natural product extracts.

HIV Assay

The anti-HIV activity of the REV/RRE binding inhibitors was evaluated according to WEISLOW *et al.*[10]. Briefly, CEM-SS cells were infected with HIV-1 RF and incubated at 37°C in the presence of serial dilutions of compounds. Six days later, XTT and *N*-methylphenazonium methosulfate were added to each well and plates were incubated for 4 hours to allow for XTT formazan production. Cell viability was quantified by light absorbance at 450 nm using a reference wavelength of 650 nm. Data were expressed as a percentage of formazan produced in test wells compared to formazan produced in wells of untreated control cells. EC_{50} values were calculated as the concentration of compound that increased the percentage of formazan production in virus-induced cells to 50% of that produced by uninfected cells. Likewise, the cytotoxicity was calculated as the concentration of compound that decreased the percentage of formazan produced in uninfected cells to 50% of that produced in untreated cells.

Cytotoxicity Assay

Cytotoxicity was assessed using a murine cell line M109 (Madison lung carcinoma 109)[11,12].

Results and Discussion

Isolation

The fractionation of the fermentation broth of *T. harzianum* WC47695 and isolation of **1** and **2** were monitored by the REV/RRE RNA binding assay, and the procedure is illustrated in Fig. 2.

Physico-chemical Properties

Harziphilone and fleephilone were each obtained as bright yellow solids. Both substances were soluble in methanol, chloroform, methylene chloride, and insoluble in hexane and water. The important physico-chemical data of these two compounds are summarized in Table 1. Their ^1H NMR spectra are reproduced in Fig. 3~4, respectively.

Fig. 2. Isolation and purification procedures of harziphilone (**1**) and fleephilone (**2**).

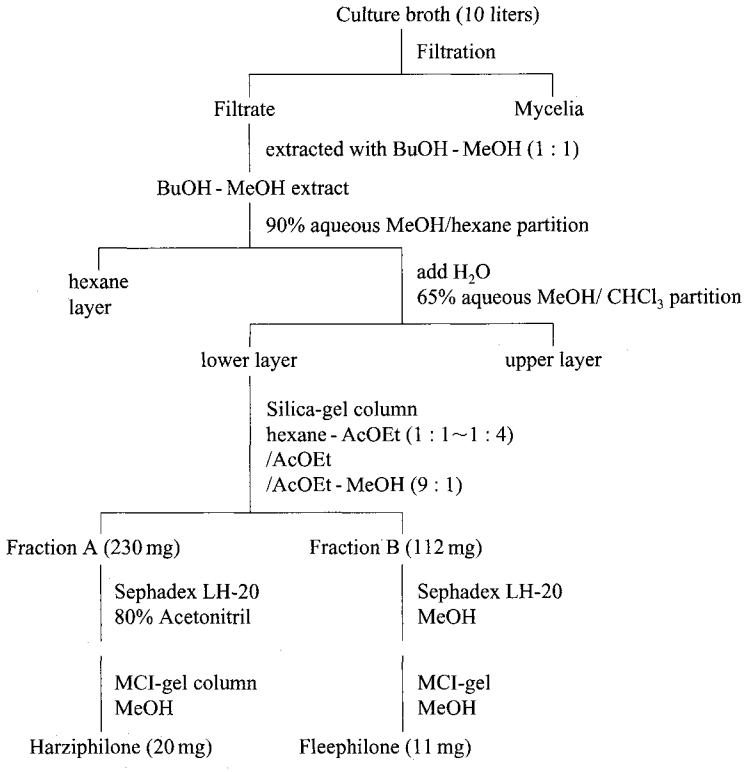

Table 1. Phisico-chemical properties of harziphilone (**1**) and fleephilone (**2**).

	1	**2**
Appearance	Yellow powder	Yellow powder
Molecular formula	$C_{15}H_{18}O_4$	$C_{24}H_{27}O_7N$
HRFAB-MS (m/z) $(M+H)^+$		
Calcd	263.1282	442.1865
Found	263.1288	442.1879
UV (MeOH) λ_{max} (nm) (ε)	228 (6752), 212 (6558), 260 (4612), 374 (4547)	209 (2252), 229 (1280), 286 (706), 389 (574)
IR (KBr) (cm^{-1})	3432, 2980, 2917, 1720, 1679, 1641, 1575, 1526, 1413, 1284, 1189, 1056, 996, 918, 863, 730	3396, 2930, 2243, 1732, 1668, 1620, 1578, 1448, 1406, 1368, 1288, 1255, 1220, 1134, 1082, 1049, 992, 914, 833
TLC[a] (Rf)	0.82	0.63
HPLC[b] (Rt)	10.2 (minutes)	8.1 (minutes)

[a] Silica-gel F_{254} aluminium sheets, CH_2Cl_2 - MeOH (90 : 10).
[b] C_{18} analytical column, Metao Solvent System[13].

Structure Elucidation

Harziphilone: (1)

High resolution FAB-MS analysis revealed that compound **1** has a molecular formula of $C_{15}H_{18}O_4$. The IR spectrum showed absorption bands at 3432 and 1642 cm^{-1}, implying that **1** should possess at least one hydroxyl group and a conjugated keto carbonyl, which was supported by the ^{13}C-signal at δ 195.9 in the ^{13}C NMR spectrum. The eight olefinic carbons between δ 105.3~161.3 indicated there are four double bonds in the structure. The ^{13}C NMR and ^1H NMR spectra further revealed the presence of two methyl groups, one methylene, one oxymethylene, one oxymethine and one oxygen-linked quaternary carbon. The above mentioned structural fragment and functional groups represented five degrees of unsaturation, thus, the remaining two degrees of unsaturation should be due to two rings in the molecule.

Detailed 1D and 2D-NMR studies including COSY, HETCOR, HMBC and COLOC (Fig. 5, Tables 2 and

Fig. 3. ^{1}H NMR spectrum of harziphilone (**1**).

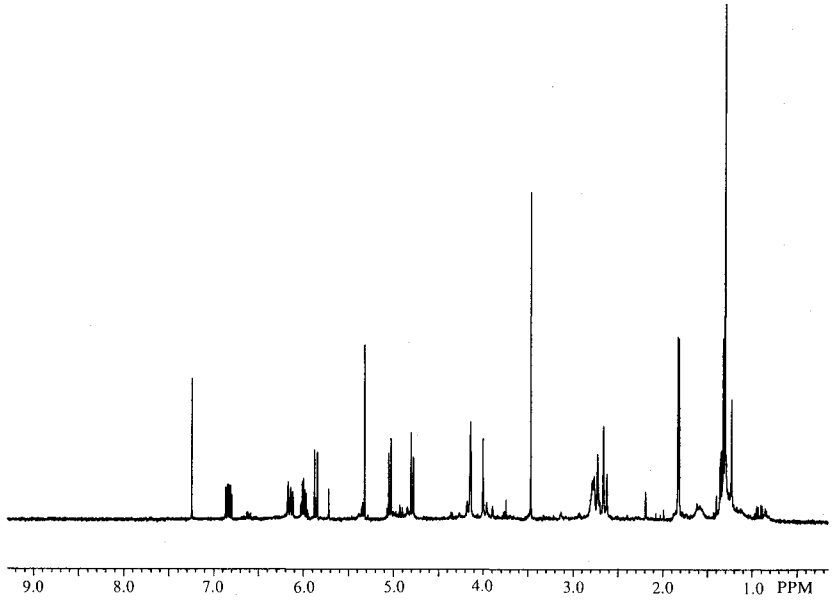

Fig. 4. ^{1}H NMR spectrum of fleephilone (**2**).

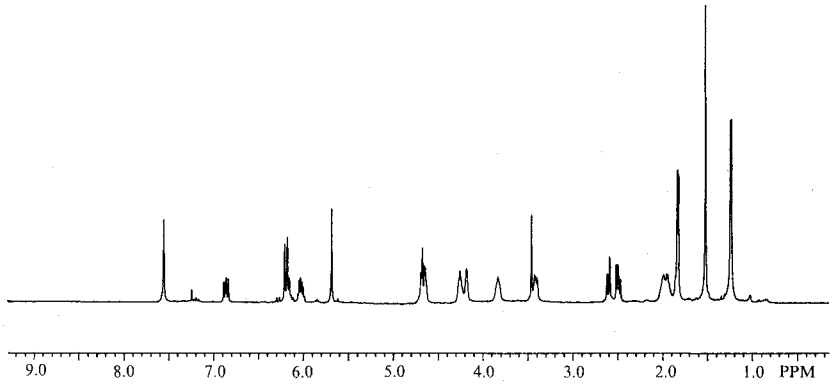

Fig. 5. Long range correlations (HMBC) of harziphilone (**1**).

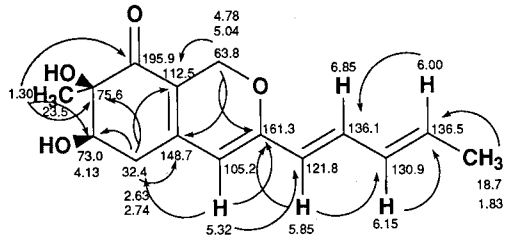

3) led to the establishment of the connectivity of the molecule, in spite of the presence of a number of quaternary carbons with few correlations. The attachment of the methyl group (C-14, δ_C 23.5; δ_H 1.30) to the quaternary carbon C-2 (δ_C 75.6) was indicated by the long-range correlation between C-2 and 14-H and supported by the signal of 14-H protons as a sharp singlet. C-2 was further connected to the keto carbonyl (C-1) on one side, and to the oxymethine (C-3) on the other side, since the long-range correlations of 14-H to C-1 at δ 195.9 and to C-3 at δ 73.0 were clearly observed. Moreover, C-2 should be linked to a oxygen atom based on its chemical shift at δ 75.6. The methylene group (C-4, δ_C 32.4; δ_{H_A} 2.63, δ_{H_B} 2.74) was placed between C-3 and the fully substituted double bond (C-4a, δ 112.5; C-8a, δ 148.7), because the 4-H_A showed the long-range correlations to C-3 and C-2 as well as to C-4a and C-8a. The double bond containing C-4a and C-8a was further linked to the oxymethylene (C-8, δ_C 63.8; δ_{H_A} 4.78, δ_{H_B} 5.04) on one side due to the long-range coupling of 8-H_B to C-4a and C-8a, and to another double bond (C-5,

Table 2. ^{1}H NMR data of harziphilone (**1**) and fleephilone (**2**) ($CDCl_3$).

Proton position	**1** δ in ppm (mult, J in Hz)	**2** δ in ppm (mult, J in Hz)
3-H	4.13 (dd, 2.3, 2.5)	
4-H	2.63 (dd, 18.8, 2.2)	5.67 (s)
	2.74 (dd, 18.9, 2.5)	
5-H	5.32 (s)	
5a-H		4.67 (d, 8.7)
6-H		4.64 (dd, 8.7, 5.6)
7-H		4.18 (m)
8-H	4.78 (dd, 12.5, 1.4)	2.00 (m)
	5.04 (dd, 12.5, 1.4)	
9-H	5.85 (d, 15.2)	3.42 (m)
		3.82 (m)
10-H	6.85 (dd, 15.1, 10.9)	7.55 (s)
11-H	6.15 (m, 14.0, 11.0, 1.4)	
12-H	6.00 (m, 13.7, 6.8)	6.20 (d, 15.2)
13-H	1.83 (d, 6.8)	6.86 (dd, 15.1, 11.0)
14-H	1.30 (s)	6.18 (dd, 14.9, 11.0)
15-H		6.02 (m, 14.9, 7.0)
16-H		1.83 (d, 6.9)
17-H		1.52 (s)
19-H		2.50 (dd, 14.3, 9.3)
		2.59 (dd, 14.4, 2.4)
20		4.21 (m)
21		1.24 (d, 6.2)

Table 3. ^{13}C NMR data of harziphilone (**1**) and fleephilone (**2**) ($CDCl_3$).

Carbon position	**1** δ in ppm	**1** Key ^{13}C-^{1}H long range correlation	**2** δ in ppm	**2** Key ^{13}C-^{1}H long range correlation
1	195.9	14-H	191.8[a]	17-H
2	75.6	14-H, 4-H_A	84.8	17-H, 4-H
3	73.0	14-H, 4-H_A	194.6[b]	17-H
4	32.4	H-5	107.0	
4a	148.7	4-H_A, 8-H_A	146.8	10-H
5	105.2		103.7	4-H, 6-H
5a			59.3	9-H_A, 10-H
6	161.3	5-H, 8-H_A, 9-H	81.6	5a-H
7			64.7	5a-H, 9-H_A
8	63.8		27.1	6-H
8a	112.5	4-H_A, 8-H_B		
9	121.8	5-H	45.1	10-H
10	136.1	12-H	149.3	9-H_A
10a			103.2	4-H, 10-H
11	130.9	9-H	157.3	6-H, 5a-H, 12-H, 13-H
12	136.5	11-H, 13-H	114.9	
13	18.7		138.6	12-H, 14-H, 15-H
14	23.5		130.8	12-H, 15-H
15			137.6	13-H
16			18.8	14-H, 15-H
17			23.9	
18			171.6	19-H_A, 19-H_B
19			43.5	21-H
20			65.1	19-H_A, 19-H_B
21			22.5	

[a,b] Interchangable.

δ 105.2; C-6, δ 161.3) on the other side to form a conjugated fragment because of the long range correlation between 5-H (δ 5.32) and C-4. This conjugated fragment (C-8a, C-4a, C-5 and C-6) must be connected to the C-1 keto carbonyl, since both double bonds have the polarized chemical shifts, which are characteristic of a conjugated keto system. The enol-ether linkage between C-8 and C-6 was confirmed by the critical long-range correlation between 8-H_B and C-6. The spin systems of the methyl protons at δ 1.83 (13-H) and the remaining four olefinic protons at δ 5.85 (9-H), 6.85 (10-H), 6.15 (11-H) and 6.00 (12-H) indicated the presence of a diene fragment with a terminal methyl group. Finally this diene side chain was connected to the olefinic carbon C-6 to form a tetraene fragment as evidenced by the long range correlations between 5-H at δ 5.32 and C-9 at δ 121.8 and between 9-H and C-6.

The relative stereochemistry of **1** was determined by ^{1}H-^{1}H coupling constants and NOE. Since the coupling constants between H-9 and H-10 and between H-11 and H-12 were 15.2 and 15.3 Hz, respectively, the double bonds in the diene side chain must be in *trans*-configuration. The strong NOE between 14-H (1.30) and 4-H_B (δ 2.74) suggested that these two groups of protons had a 1,3-diaxial relationship, and they were obviously on the same side of the ring. The small coupling constants between 3-H and 4-H_A (2.2 Hz) and between 3-H and 4-H_B (2.5 Hz) indicated that 3-H should be equatorial or quasi-equatorial, which was well supported by the positive NOEs between 3-H and 14-H, as well as between 3-H and 4-H_B. As a result, the hydroxyl at C-3 should be axial and *trans* to the methyl group at C-2. Thus, the relative stereochemistry of **1** was established as shown in Fig. 1. The absolute stereochemistry of the asymmetric centers (C-2 and C-3) was, however, not determined due to insufficient quantity of the material.

Fleephilone (2)

Compound **2** showed a chemical composition of $C_{24}H_{27}O_7N$ by high resolution FAB mass spectrometry, indicating an unsaturation number of twelve. An absorption maximum at 389 in the UV spectrum suggested the extended conjugation system. The IR spectrum exhibited characteristic absorptions of hydroxyl (3400 cm^{-1}), ester carbonyl (1732 cm^{-1}), highly conjugated carbonyl (1620 and 1578 cm^{-1}) groups. The ^{13}C NMR

spectrum consisting of 24 signals confirmed the presence of two conjugated keto carbonyl (δ 194.6, 191.8) groups and one ester carbonyl (δ 171.6) group. Ten olefinic carbon signals between δ 103.2~157.3 implying five double bonds in the structure. In addition, signals due to the following functional groups were observed in NMR spectra: three methyl groups, three methylene groups, four methine groups and one quaternary carbon. Moreover, there should be four rings in the molecule due to the remaining four degrees of unsaturation. The key connectivity of compound **2** was derived mainly from the careful studies of its COSY, HETCOR and HMBC data (Tables 2, 3; Fig. 6). The proton signals of the methyl at δ 1.52 (H-17) appeared as a singlet, indicating this methyl is attached to a quaternary carbon, namely C-2, due to the long-range coupling of 17-H to C-2 at δ 84.8. The quaternary C-2 is placed between two keto carbonyls (C-1, δ 191.8 and C-3, δ 194.6), because the methyl protons showed long-range couplings to both C-1 and C-3. Both these keto carbonyls should be linked to double bonds to form the conjugated keto segments, which was indicated by their ^{13}C NMR chemical shifts as well as IR spectrum. The fragment consisting of C-3, C-4 and C-4a was supported by the polarized chemical shifts of C-4 (δ 107.0) and C-4a (δ 146.8) due to the electron pulling effect of the keto carbonyl, and was proven by the long-range correlation between the olefinic proton at δ 5.67 (4-H) and C-2. Similarly, the fragment containing C-1, C-10a and C-10, was supported by the polarized chemical shifts of C-10a (δ 103.2) and C-10 (δ 149.3). The expected downfield shift of H-10 (δ 7.55) was also in agreement with the structure of this fragment. The linkage between C-10a and C-4a (A-B ring connection) was obvious due to the long-range correlations between 10-H and C-4a as well as between 4-H and C-10a. The double bond of C-4 and C-4a was further connected to another double bond consisting of C-5 and C-11 because of the observation of the long-range correlation between H-4 and C-5 (δ 103.7). Furthermore, the position of C-5a as a bridgehead of the B, C and D rings was confirmed by the long range coupling of C-5a (δ 59.3) to 10-H in B-ring and the long range couplings of 5a-H (δ 4.67) to C-11 (δ 157.3) in D-ring as well as C-6 (δ 81.6) and C-7 (δ 64.7) in C-ring. The placement of one nitrogen atom as the other bridgehead between B and C-rings was suggested by the chemical shifts of the adjacent carbons C-5a (δ 59.3), C-10 (δ 149.3) and C-9 (δ 45.1). The construction of the remaining building blocks (C-6, C-7, C-8 and C-9) of C-ring was indicated by their proton-spin systems, and proven by HMBC correlations of the corresponding carbons and protons. The enol-ether linkage between C-11 and C-6 in D-ring was confirmed by the critical long range coupling between 6-H (δ 4.64) and C-11. Similar to the structure of **1**, compound **2** should bear a diene side chain with a terminal methyl group, which is implied by the spin systems of the olefinic protons at δ 6.20 (12-H), 6.86 (13-H), 6.18 (14-H) and 6.02 (15-H) and the methyl protons at δ 1.83 (16-H). The attachment of this diene side chain to C-11 was derived by the long range correlations of 12-H and 13-H to C-11. In addition to the above described core fragment (Fig. 6), the following remaining functionalities: one carbonyl, one methyl, one methylene and one oxymethine group, can be assigned to one side fragment, designated as fragment A (Fig. 6). In fragment A, the carbonyl group (C-18, δ 171.6) must be connected to the methylene (C-19) based on the chemical shift of C-19 (δ 43.5) and the long range couplings of H-19$_A$ (δ 2.50) and H-19$_B$ (δ 2.59) to C-18. The sequence of the linkage from C-19 to C-21 was

Fig. 6. Long range correlations (HMBC) of fleephilone (**2**).

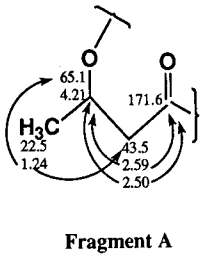

Fragment A

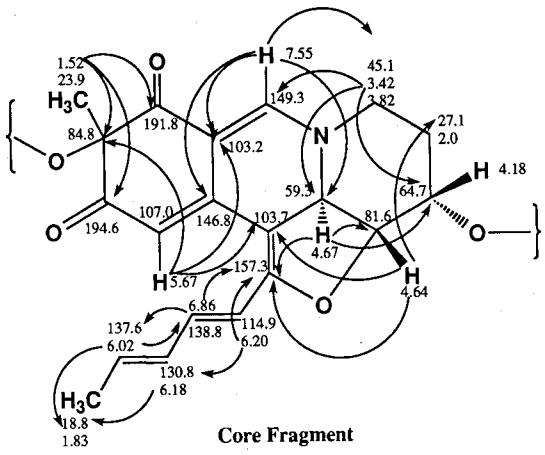

Core Fragment

indicated by the proton spin systems and proven by the HMBC correlations. In terms of the attachment between the fragment A and the core fragment, there were the following four possible linkages: ester linkage between C-18 and C-2; ester linkage between C-18 and C-7; ether linkage between C-20 and C-2; ether linkage between C-20 and C-7. In order to determine how the fragment A was attached to the core fragment in this molecule, *in situ* acylation with TAI (Trichloroacetyl isocyanate) agent[14] was carried out. The changes in the ^{1}H NMR spectrum after the addition of the reagent were carefully observed and analyzed. Compared to the corresponding signals of the parent compound, the signals of H-7 and H-20 of acylated compound were significantly shifted downfield by 1.12 and 1.18 ppm, respectively. This result clearly indicated that free hydroxyl groups are attached to C-20 and C-7. In contrast, no change was observed on the chemical shift of methyl protons (17-H). Based on the above evidence, the carbonyl C-18 must be linked to the hydroxyl group at C-2 to form a ester linkage as shown in Fig. 1. The downfield shift of C-2 by 9.2 ppm, compared to that of the C-2 of **1**, which is bearing a free hydroxyl group, also supported that C-2 of **2** should be the carrier of the fragment A.

The relative stereochemistry of C-5a, C-6 and C-7 was determined by NOE experiments and the ^{1}H-^{1}H coupling constants. The larger coupling constant between 6-H and 5a-H ($J_{a,a}=8.7$ Hz) implied that these two protons had a diaxial (*trans*) relation, which was in agreement with the fact that no NOE was observed between them. A *cis* configuration between 6-H and 7-H was indicated by their relative small coupling constant ($J_{a,e}=5.6$ Hz), and proven by the positive NOE between these two protons. The structure of **2** was thus established as shown in Fig. 1. However, the quantity of this compound available was insufficient to enable the absolute stereochemistry of the asymmetric centers (C-2, C-6, C-7, C-5a and C-20) to be established by chemical degradation study.

Compound **1** probably belongs to the class of hydrogenated azaphilones, while **2** seems to be structurally related to azaphilone with a 3-hydroxyl butanoyl moiety. Biogenetically they may also be related to azaphilones.

Biological Activity

Compounds **1** and **2** inhibited the binding of REV-protein to [^{33}P] labeled RRE RNA with IC_{50} values of 2.0 μM and 7.6 μM, respectively. The compounds were also evaluated for anti-HIV activity using an XTT dye reduction assay[10]. Both compounds did not protect CEM-SS cells from acute HIV-1 infection at concentrations up to 200 μg/ml against acute HIV-1 infection. In addition, **1** demonstrated cytotoxicity at 38 μM against the murine tumor cell line M-109. Compound **2** was not cytotoxic at 227 μM in this system.

Acknowledgments

We thank J. YACOBUCCHI and J. GUSS for instrumentation support; Ms. K. NEDDERMAN and Dr. I. BURSUKER for cytotoxicity testing; Drs. D. VYAS, S. FORENZA, J. O'SULLIVAN and J. TRIMBLE for helpful discussion.

References

1) ZAPP, M. L.; T. J. HOPE, T. G. PARSLOW & M. R. GREEN: Oligomerization and RNA binding domains of the type 1 human immunodeficiency virus Rev protein: A dual function for an arginine-rich binding motif. Proc. Natl. Acad. Sci. U.S.A. 88: 7734~7738, 1991
2) BARTEL, D. P; M. L. ZAPP, M. R. GREEN & J. W. SZOSTAK: HIV-1 Rev regulation involves recognition of non-Watson-Crick base pairs in viral RNA. Cell 67: 529~536, 1991
3) DALY, T. J.; K. S. COOK, G. S. GRAY, T. E. MALONE & J. R. RUSCHE: Specific binding of HIV-1 recombinant Rev protein to the Revresponsive element *in vitro*. Nature 342: 816~819, 1989
4) BARNETT, H. L. & B. B. HUNTER: Illustrated Genera of Imperfect Fungi, 4th edition. McMillan Publishing Co., New York, 1972
5) RIFAI, M. A.: A revision of the genus *Trichoderma*. Mycological Papers 116: 1~56, 1969
6) ZAPP, M. L. & M. R. GREEN: Sequence-specific RNA binding by the HIV-1 Rev protein. Nature 342: 714~716, 1989
7) ZAPP, M. L.; S. STERN & M. R. GREEN: Small molecules that selectively block RNA binding of HIV-1 Rev protein inhibit Rev function and viral production. Cell 74: 969~978, 1993
8) HEAPHY, S.; C. DINGWALL, I. ERNBERG, M. J. GAIT, S. M. GREEN, J. KARN, A. D. LOWE, M. SINGH & M. A. SKINNER: HIV-1 Regulator of virion expression (Rev) protein binds to an RNA stem-loop structure located within the Rev response element region. Cell 60: 685~693, 1990
9) SCHROEDER, H. C.; H. USHIJIMA, A. BEK, H. MERZ, K. PFEIFER & W. E. G. MULLER: Inhibition of formation of Rev-RRE complex by pyronin Y. Antiviral Chemistry and Chemotherapy 4(2): 103~111, 1993
10) WEISLOW, O. S.; R. KISER, D. L. FINE, J. BADER, R. J. SHOWMAKER & M. R. BOYD: New soluble-formazan assay for HIV-1 cytopathic effects: Application to high-flux screening of synthetic and natural products for AIDS-antiviral activity. J. Natl. Can. Inst. 81: 577~586, 1989
11) MARKS, T. A.; R. J. WOODMAN, R. I. GERAN, L. H. BILLUPS & R. M. MADISON: Characterization and responsiveness of the Madison 109 lung carcinoma to various anti-tumor agents. Cancer Threat. 61: 1459~1470, 1977
12) MCBRIEN, K. D.; R. BERRY, S. E. LOWE, K. NEDDERMANN, I. BURSUKER, S. HUANG, S. E. KLOHR & J. E. LEET: Rakicidins, new cytotoxic lipopeptides from *Micro-*

monospora sp.: Fermentation, isolation and characterization. J. Antibiotics 48: 1446~1452, 1995

13) HOOK, D. J.; C. F. MORE, J. J. YACOBUCCI, G. DUBAY & S. O'CONNOR: Intergrated biological-physicochemical system for the identification of antitumor compounds in fermentation broths. J. Chromatography 385: 99~108, 1987

14) SAMEK, Z. & M. BUDESINSKY: *in situ* Reactions with trichloroacetyl isocyanate and their application to structural assignment of hydroxy compounds by ^{1}H NMR spectroscopy: A general comment. Collection Czechoslov. Chem. Commun. 44: 558~588, 1979